A

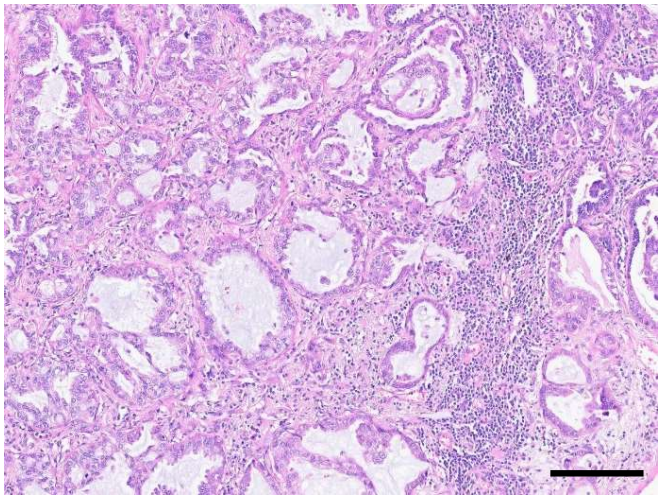

B

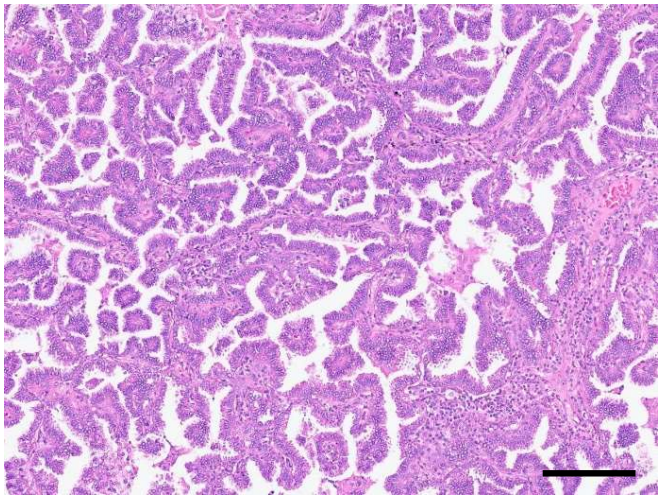

C

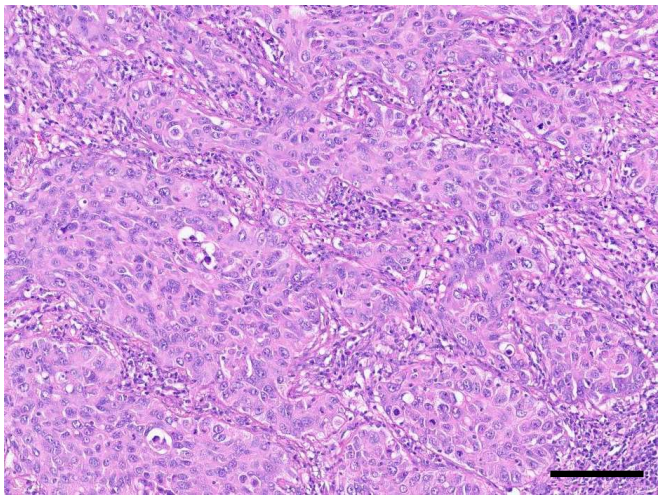

D

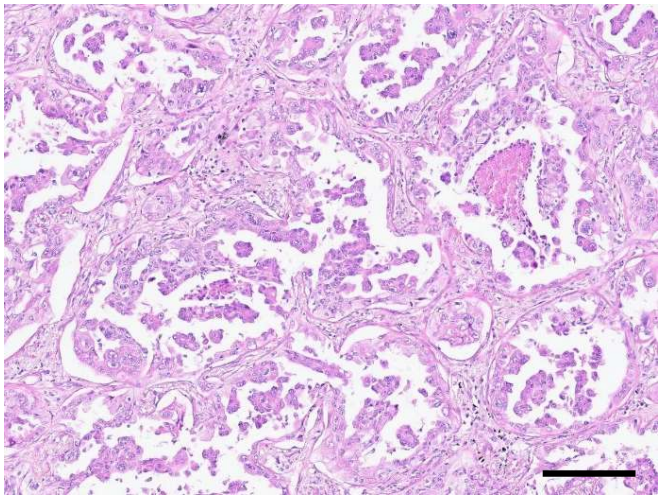

E

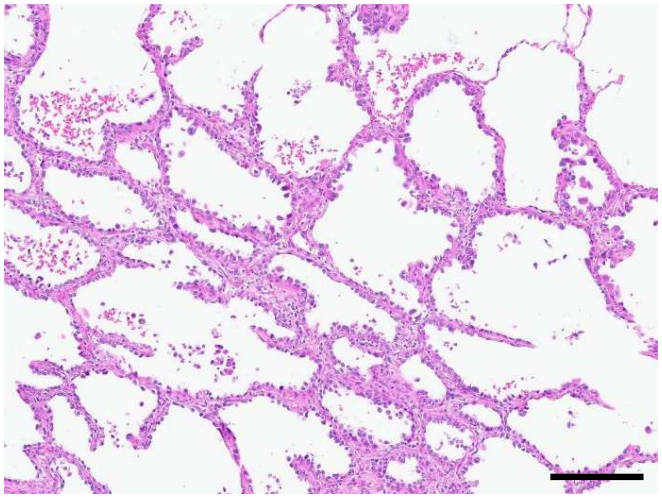

Fig. S1

Fig S1 Typical histologic patterns of lung adenocarcinoma from representative cases according to the IASLC/ATS/ERS classification (hematoxylin and eosin staining; magnification, ×100).

A Acinar pattern (from KNUCH14) shows round to oval-shaped malignant glands invading a fibrous stroma. **B** Papillary pattern (from KNUCH22) consists of malignant cuboidal to columnar tumor cells growing along fibrovascular cores. **C** Solid pattern (from KNUCH02) is composed of cohesive sheets of tumor cells with abundant cytoplasm and predominantly vesicular nuclei, often containing conspicuous nucleoli. **D** Micropapillary pattern (from KNUCH13) is characterized by small papillary clusters of glandular tumor cells floating within alveolar spaces, most lacking fibrovascular cores. **E** Lepidic pattern (from KNUCH13) shows proliferation of type II pneumocytes and Clara cells lining the preserved alveolar walls. Scale bar: 100μm.

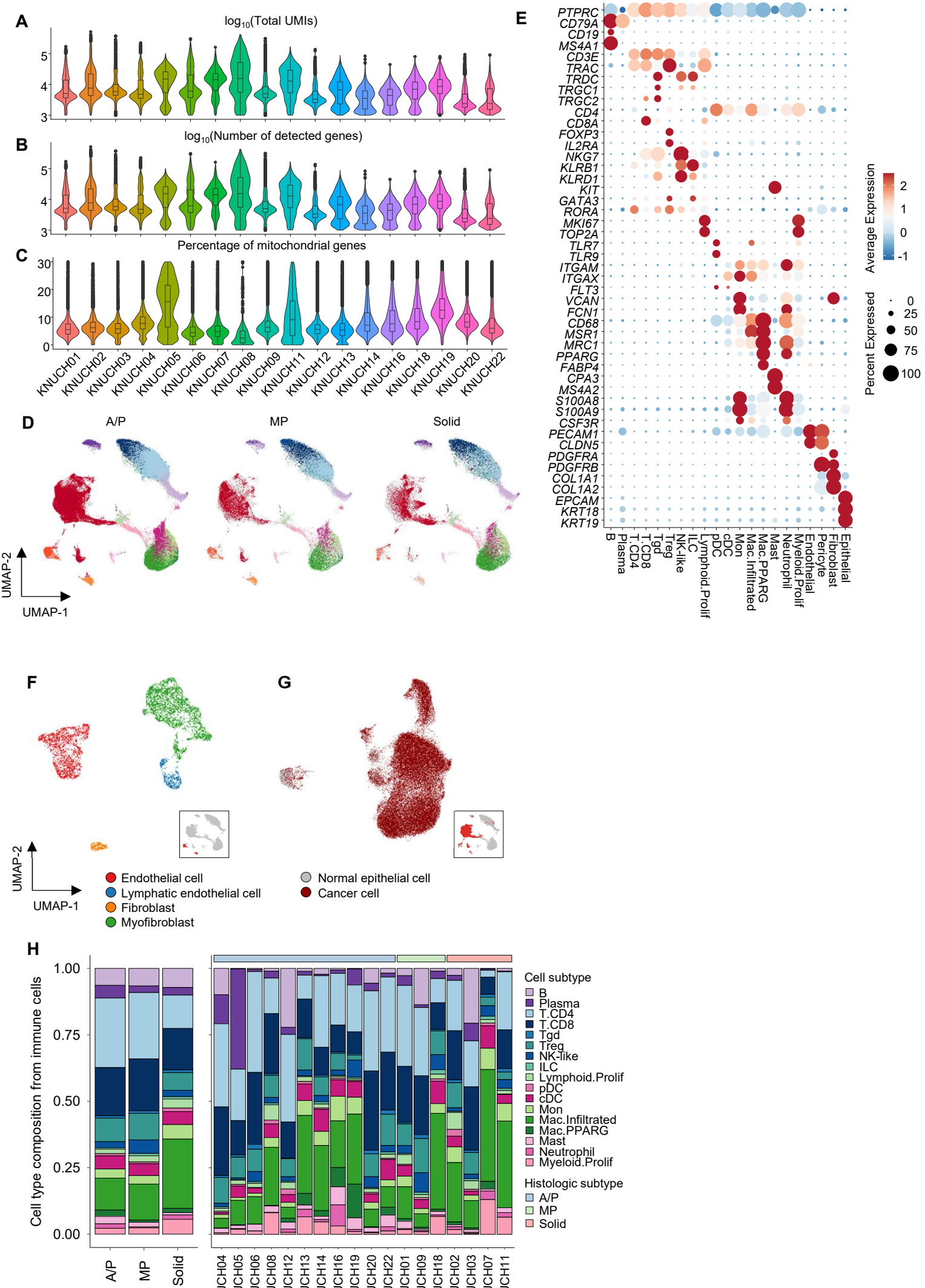
A
log10(Total UMIs)
B
log10(Number of detected genes)
C
Percentage of mitochondrial genes
KNUCH01
KNUCH02
KNUCH03
KNUCH04
KNUCH05
KNUCH06
KNUCH07
KNUCH08
KNUCH09
KNUCH11
KNUCH12
KNUCH13
KNUCH14
KNUCH16
KNUCH18
KNUCH19
KNUCH20
KNUCH22
D
A/P
MP
Solid
UMAP-2
UMAP-1
E
PTPRC
CD79A
CD19
MS4A1
CD3E
TRAC
TRDC
TRGC1
TRGC2
CD4
CD8A
FOXP3
IL2RA
NKG7
KLRB1
KLRD1
KIT
GATA3
RORA
MKI67
TOP2A
TLR7
TLR9
ITGAM
ITGAX
FLT3
VCAN
FCN1
CD68
MSR1
MRC1
PPARG
FABP4
CPA3
MS4A2
S100A8
S100A9
CSF3R
PECAM1
CLDN5
PDGFRA
PDGFRB
COL1A1
COL1A2
EPCAM
KRT18
KRT19
B
Plasma
T.CD4
T.CD8
Tgd
Treg
NK-like
ILC
Lymphoid.Prolif
pDC
cDC
Mon
Mac.Infiltrated
Mac.PPARG
Mast
Neutrophil
Myeloid.Prolif
Endothelial
Pericyte
Fibroblast
Epithelial
Average Expression
Percent Expressed
F
G
UMAP-2
UMAP-1
Endothelial cell
Lymphatic endothelial cell
Fibroblast
Myofibroblast
Normal epithelial cell
Cancer cell
H
Cell type composition from immune cells
A/P
MP
Solid
KNUCH04
KNUCH05
KNUCH06
KNUCH08
KNUCH12
KNUCH13
KNUCH14
KNUCH16
KNUCH19
KNUCH20
KNUCH22
KNUCH01
KNUCH09
KNUCH18
KNUCH02
KNUCH03
KNUCH07
KNUCH11
Cell subtype
B
Plasma
T.CD4
T.CD8
Tgd
Treg
NK-like
ILC
Lymphoid.Prolif
pDC
cDC
Mon
Mac.Infiltrated
Mac.PPARG
Mast
Neutrophil
Myeloid.Prolif
Histologic subtype
A/P
MP
Solid

Fig. S2

Fig. S2 Quality control metrics and cellular composition of the LUAD TME.

A–C Violin plots depicting cell quality control measures: $\log_{10}$(total UMIs) (**A**), $\log_{10}$(number of detected genes) (**B**) and percentage of reads mapped to the mitochondrial genome (**C**). **D** UMAP plots showing the distribution of cell types across different histologic subtype groups. **E** Dot plot showing marker gene expression patterns across cell types. Dot size represents the percentage of cells expressing the gene, while color intensity indicates average expression level. **F,G** UMAP plots of endothelial cells and fibroblasts (**F**) and normal/malignant epithelial cells (**G**). Insets show the location of these cells in the overall UMAP from Fig. 1B. **H** Stacked bar plot illustrating the proportional composition of immune cell types across different samples.

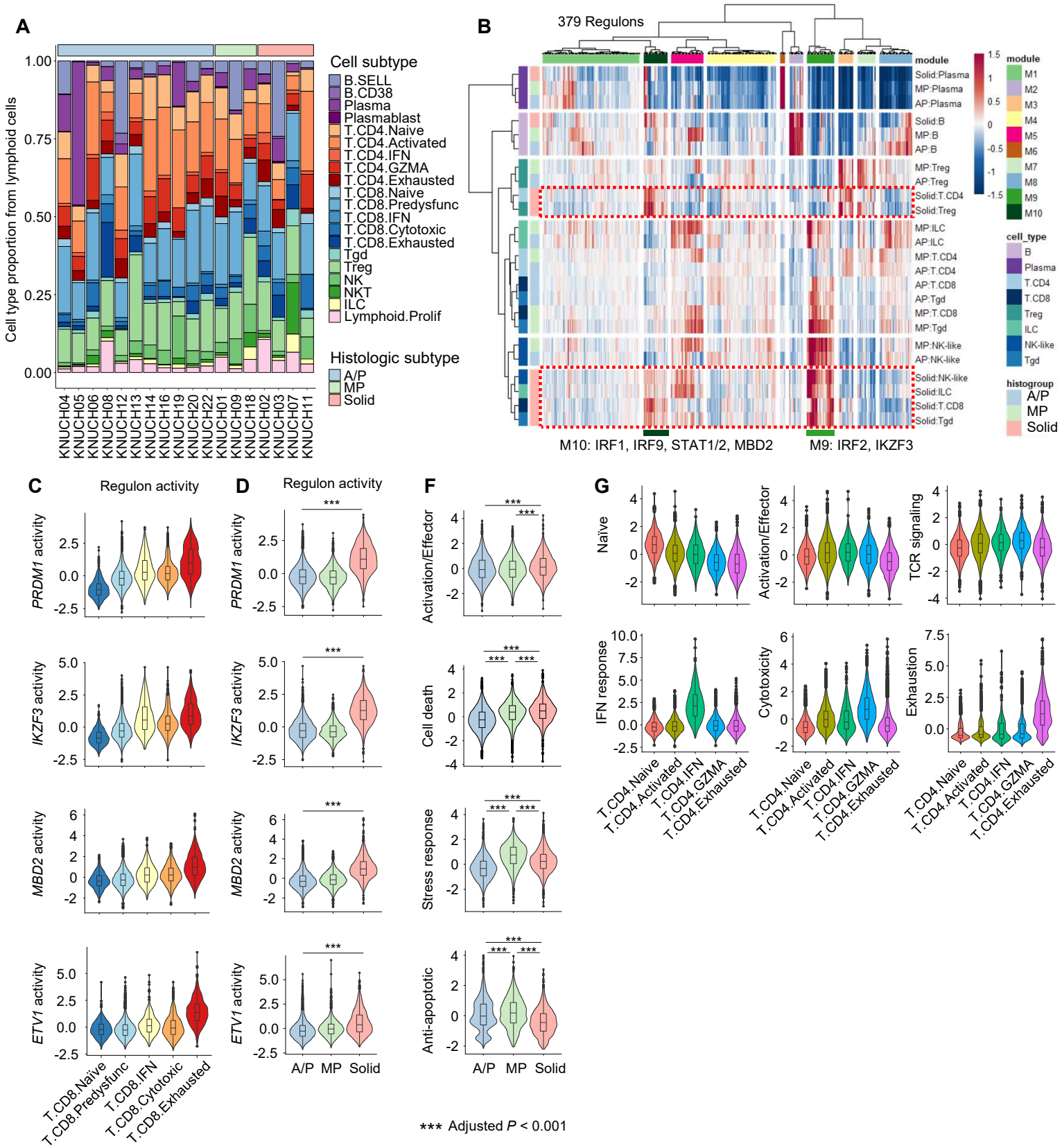
A
Cell type proportion from lymphoid cells
1.00
0.75
0.50
0.25
0.00
KNUCH04
KNUCH05
KNUCH06
KNUCH08
KNUCH12
KNUCH13
KNUCH14
KNUCH16
KNUCH19
KNUCH20
KNUCH22
KNUCH01
KNUCH09
KNUCH18
KNUCH02
KNUCH03
KNUCH07
KNUCH11
Cell subtype
B.SELL
B.CD38
Plasma
Plasmablast
T.CD4.Naive
T.CD4.Activated
T.CD4.IFN
T.CD4.GZMA
T.CD4.Exhausted
T.CD8.Naive
T.CD8.Predysfunc
T.CD8.IFN
T.CD8.Cytotoxic
T.CD8.Exhausted
Tgd
Treg
NK
NKT
ILC
Lymphoid.Prolif
Histologic subtype
A/P
MP
Solid
B
379 Regulons
module
Solid:Plasma
MP:Plasma
AP:Plasma
Solid:B
MP:B
AP:B
MP:Treg
AP:Treg
Solid:T.CD4
Solid:Treg
MP:ILC
AP:ILC
MP:T.CD4
AP:T.CD4
AP:T.CD8
AP:Tgd
MP:T.CD8
MP:Tgd
MP:NK-like
AP:NK-like
Solid:NK-like
Solid:ILC
Solid:T.CD8
Solid:Tgd
1.5
1
0.5
0
-0.5
-1
-1.5
module
M1
M2
M3
M4
M5
M6
M7
M8
M9
M10
cell_type
B
Plasma
T.CD4
T.CD8
Treg
ILC
NK-like
Tgd
histogroup
A/P
MP
Solid
M10: IRF1, IRF9, STAT1/2, MBD2
M9: IRF2, IKZF3
C
Regulon activity
PRDM1 activity
IKZF3 activity
MBD2 activity
ETV1 activity
T.CD8.Naive
T.CD8.Predysfunc
T.CD8.IFN
T.CD8.Cytotoxic
T.CD8.Exhausted
D
Regulon activity
PRDM1 activity
IKZF3 activity
MBD2 activity
ETV1 activity
***
A/P
MP
Solid
F
Activation/Effector
Cell death
Stress response
Anti-apoptotic
***
A/P
MP
Solid
G
Naive
Activation/Effector
TCR signaling
IFN response
Cytotoxicity
Exhaustion
T.CD4.Naive
T.CD4.Activated
T.CD4.IFN
T.CD4.GZMA
T.CD4.Exhausted
*** Adjusted P < 0.001
E
Lymphoid.Prolif
ILC
NKT
NK
Treg
Tgd
T.CD8.Exhausted
T.CD8.Cytotoxic
T.CD8.IFN
T.CD8.Predysfunc
T.CD8.Naive
T.CD4.Exhausted
T.CD4.GZMA
T.CD4.IFN
T.CD4.Activated
T.CD4.Naive
Plasmablast
Plasma
B.CD38
B.SELL
CD79A
MS4A1
SELL
CD38
PRDM1
SDC1
CD3D
CD3G
TRAC
CCR7
TCF7
LEF1
CD28
CD44
CD69
ISG15
ISG20
GZMK
GZMA
GZMB
PDCD1
TIGIT
LAG3
HAVCR2
CTLA4
FOXP3
IL2RA
TRDC
TRGC1
TRGC2
ZBTB16
NKG7
KLRB1
KLRD1
KLRF1
KIT
GATA3
MKI67
TOP2A
Average Expression
1.0
0.0
-1.0
Percent Expressed
0
25
50
75

Fig. S3

Fig. S3 Transcriptional profiling of lymphoid cell subtypes and T cell functionality across histologic subtype groups.

A Stacked bar plot illustrating the proportional composition of lymphoid cell subtypes across different samples. **B** Heatmap showing the activity of 379 regulons across lymphoid cell subtypes and histologic subtype groups (A/P, MP, Solid). Columns represent regulons, rows represent cell types grouped by histologic subtypes and colors indicate regulon activity levels. **C,D** Violin plots showing T cell exhaustion-associated regulon activity (PRDM1, IKZF3, MBD2, ETV1) across $CD8^+$ T cell states (**C**) and histologic subtype groups (**D**). **E** Dot plot showing average expression and percentage of cells expressing marker genes for lymphoid cell subtypes. Color intensity represents average expression, while dot size indicates the percentage of cells expressing each gene. **F** Violin plots comparing four signatures (activated/effector, cell death, stress response and anti-apoptotic) across histologic subtype groups (A/P, MP and Solid). **G** Violin plots comparing signature scores of curated gene sets related to $CD4^+$ T cell functionality.

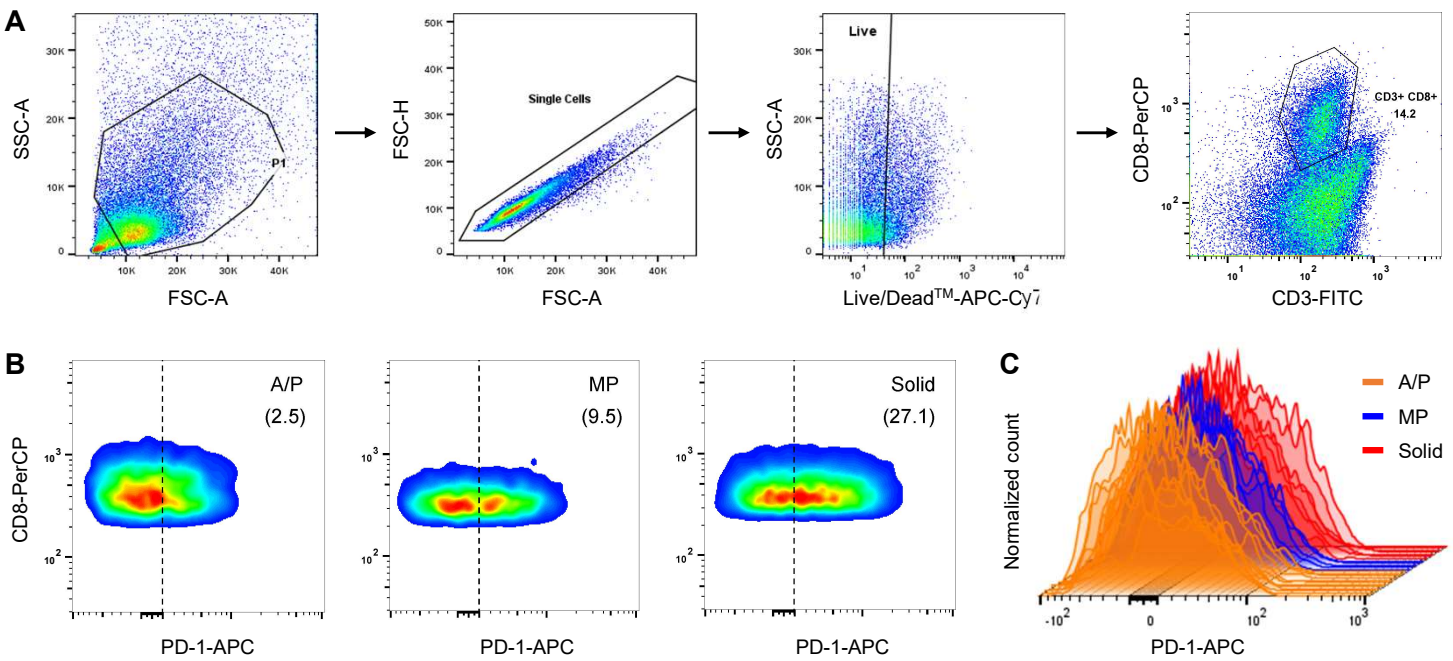

Fig. S4 Flow cytometric analysis of PD-1 expression in CD8+⁺ T cells across LUAD subtypes.

A Gating strategy for $CD8^+$ T cells. **B** Density plots illustraging the abundance of PD-1-expressing $CD8^+$ T cells in representative cases of each subtype. **C** Histogram illustrating $PD\text{-}1^+CD8^+$ T cells across histologic subtypes of LUAD. Plot was created using FlowJo software.

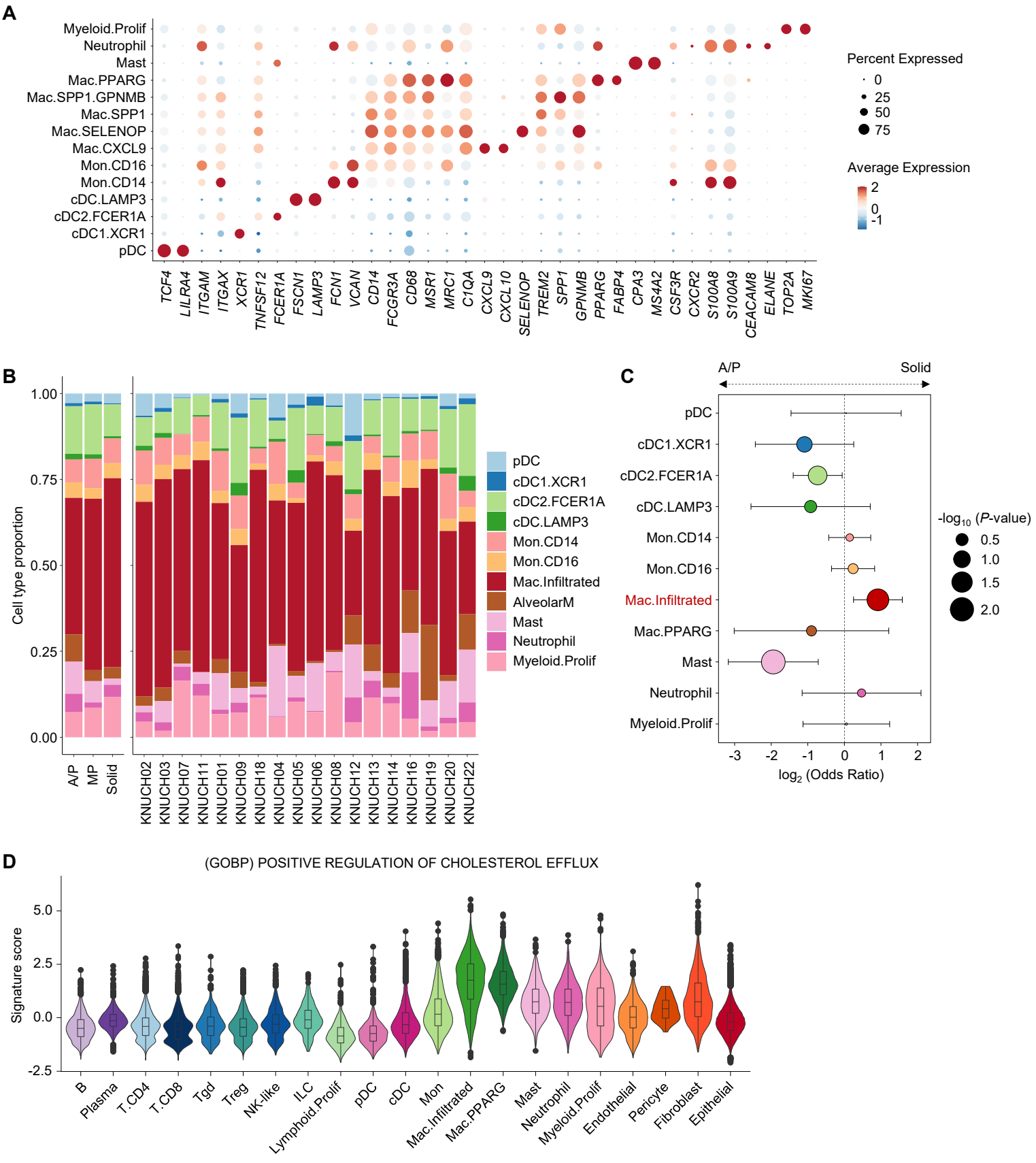
A
Myeloid.Prolif
Neutrophil
Mast
Mac.PPARG
Mac.SPP1.GPNMB
Mac.SPP1
Mac.SELENOP
Mac.CXCL9
Mon.CD16
Mon.CD14
cDC.LAMP3
cDC2.FCER1A
cDC1.XCR1
pDC
TCF4 LILRA4 ITGAM ITGAX XCR1 TNFSF12 FCER1A FSCN1 LAMP3 FCN1 VCAN CD14 FCGR3A CD68 MSR1 MRC1 C1QA CXCL9 CXCL10 SELENOP TREM2 SPP1 GPNMB PPARG FABP4 CPA3 MS4A2 CSF3R CXCR2 S100A8 S100A9 CEACAM8 ELANE TOP2A MKI67
Percent Expressed
0
25
50
75
Average Expression
2
0
-1
B
Cell type proportion
1.00
0.75
0.50
0.25
0.00
A/P MP Solid
KNUCH02 KNUCH03 KNUCH07 KNUCH11 KNUCH01 KNUCH09 KNUCH18 KNUCH04 KNUCH05 KNUCH06 KNUCH08 KNUCH12 KNUCH13 KNUCH14 KNUCH16 KNUCH19 KNUCH20 KNUCH22
pDC
cDC1.XCR1
cDC2.FCER1A
cDC.LAMP3
Mon.CD14
Mon.CD16
Mac.Infiltrated
AlveolarM
Mast
Neutrophil
Myeloid.Prolif
C
A/P
Solid
pDC
cDC1.XCR1
cDC2.FCER1A
cDC.LAMP3
Mon.CD14
Mon.CD16
Mac.Infiltrated
Mac.PPARG
Mast
Neutrophil
Myeloid.Prolif
-3 -2 -1 0 1 2
log2 (Odds Ratio)
-log10 (P-value)
0.5
1.0
1.5
2.0
D
(GOBP) POSITIVE REGULATION OF CHOLESTEROL EFFLUX
Signature score
5.0
2.5
0.0
-2.5
B Plasma T.CD4 T.CD8 Tgd Treg NK-like ILC Lymphoid.Prolif pDC cDC Mon Mac.Infiltrated Mac.PPARG Mast Neutrophil Myeloid.Prolif Endothelial Pericyte Fibroblast Epithelial

Fig. S5

Fig. S5 Characterization and differential abundance of myeloid cell subtypes across histologic subtype groups.

A Dot plot showing average expression and percentage of cells expressing marker genes for myeloid cell subtypes. **B** Stacked bar plots depicting the proportional distribution of myeloid cell subtypes across histologic subtype groups (left) and individual samples (right). **C** Differential abundance analysis of myeloid cell subtypes between A/P and Solid groups using MASC. The x-axis represents $\log_2$(odds ratio), dot size indicates $-\log_{10}$(*P*-value) and error bars indicate 95% confidence intervals. **D** Violin plots showing cholesterol efflux metabolism signature scores across all cell types.

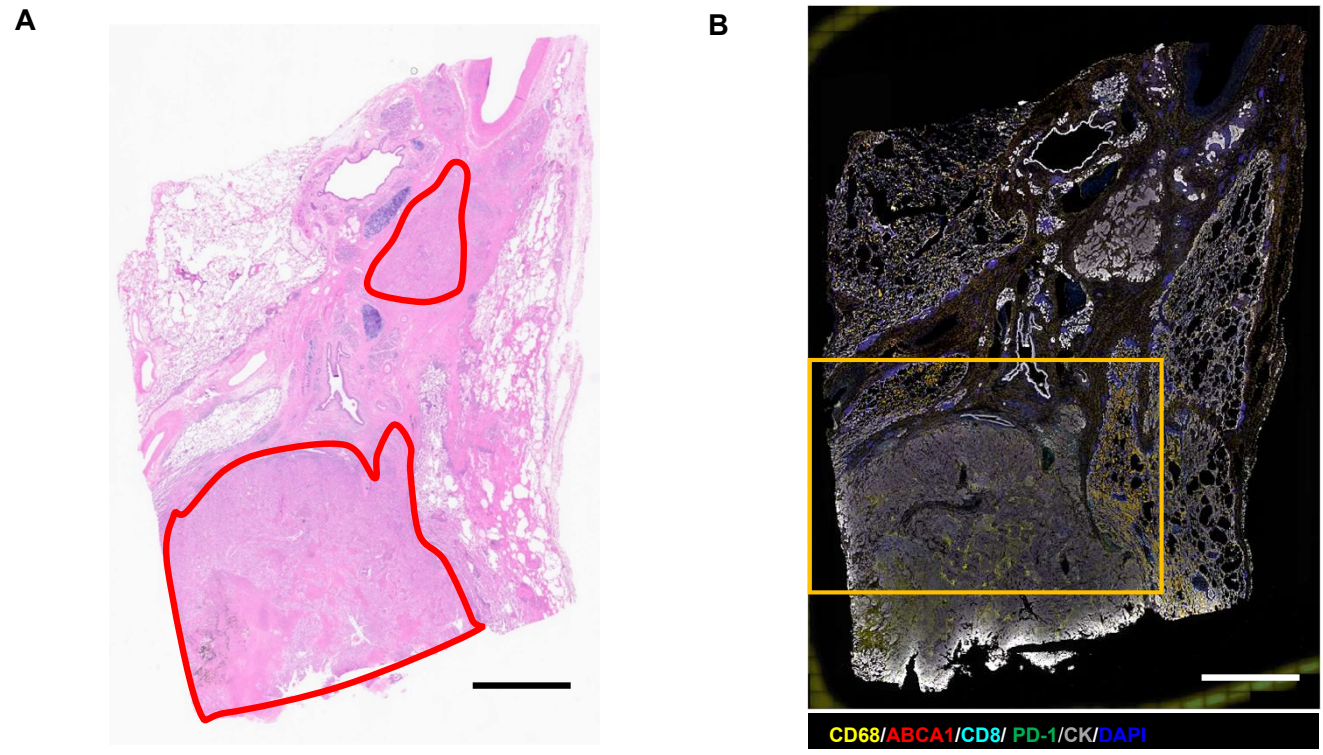

Fig. S6

D

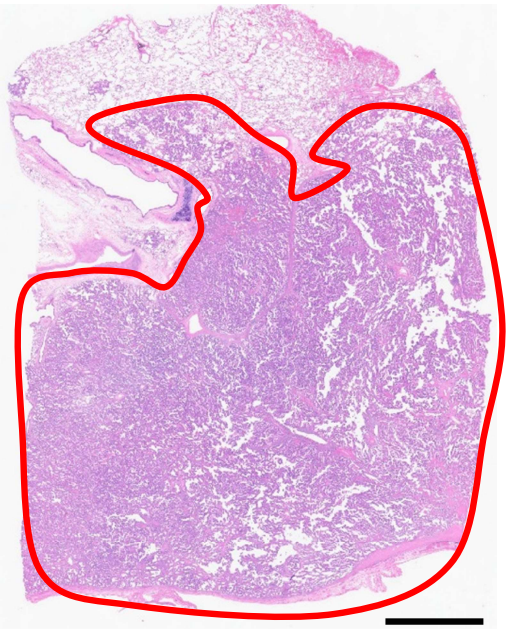

E

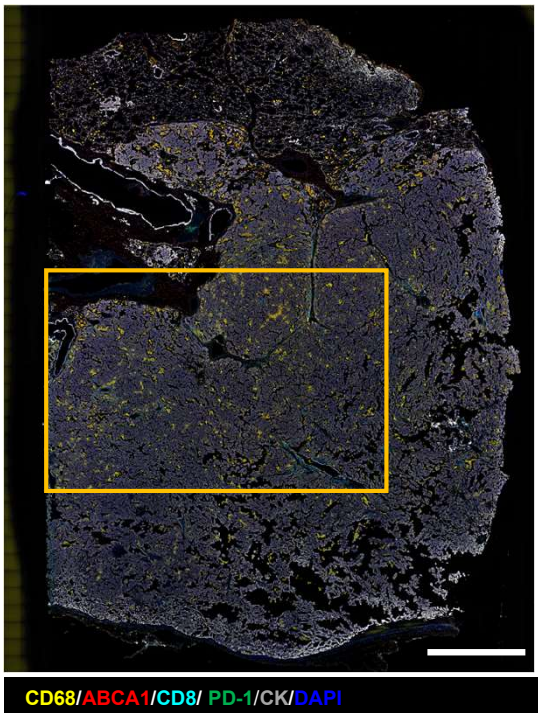

F

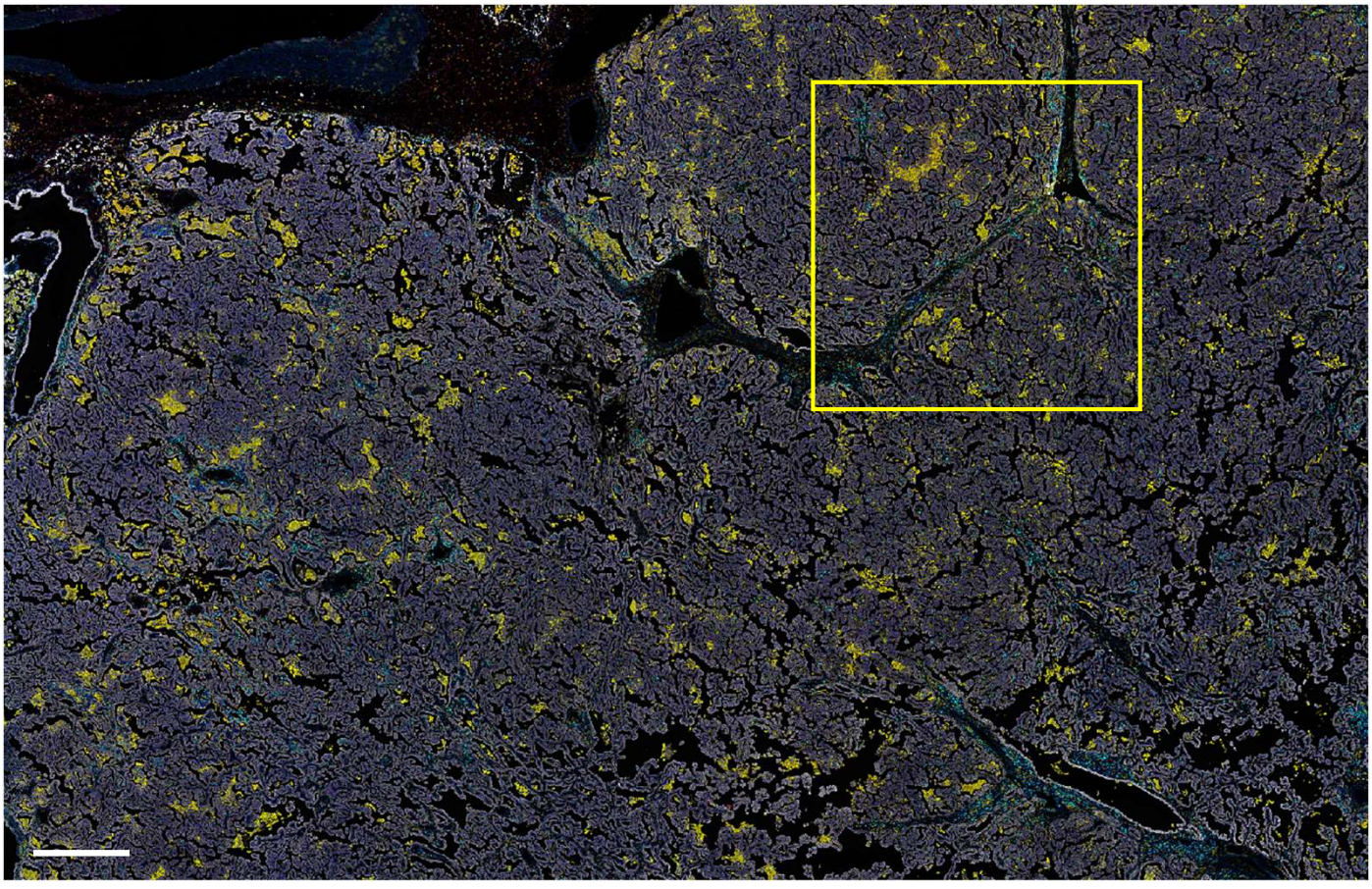

Fig. S6 (Cont'd)

G

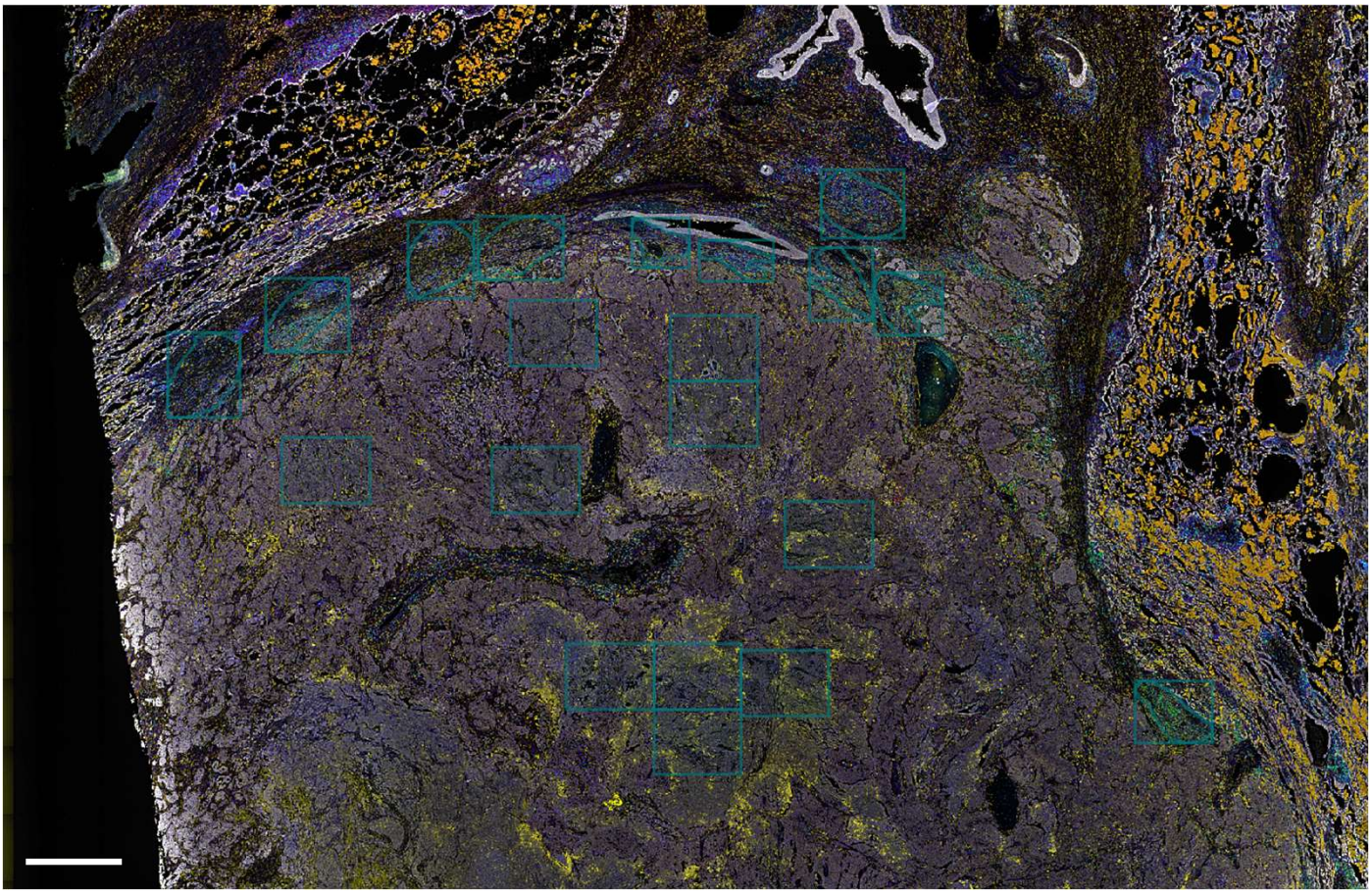

H

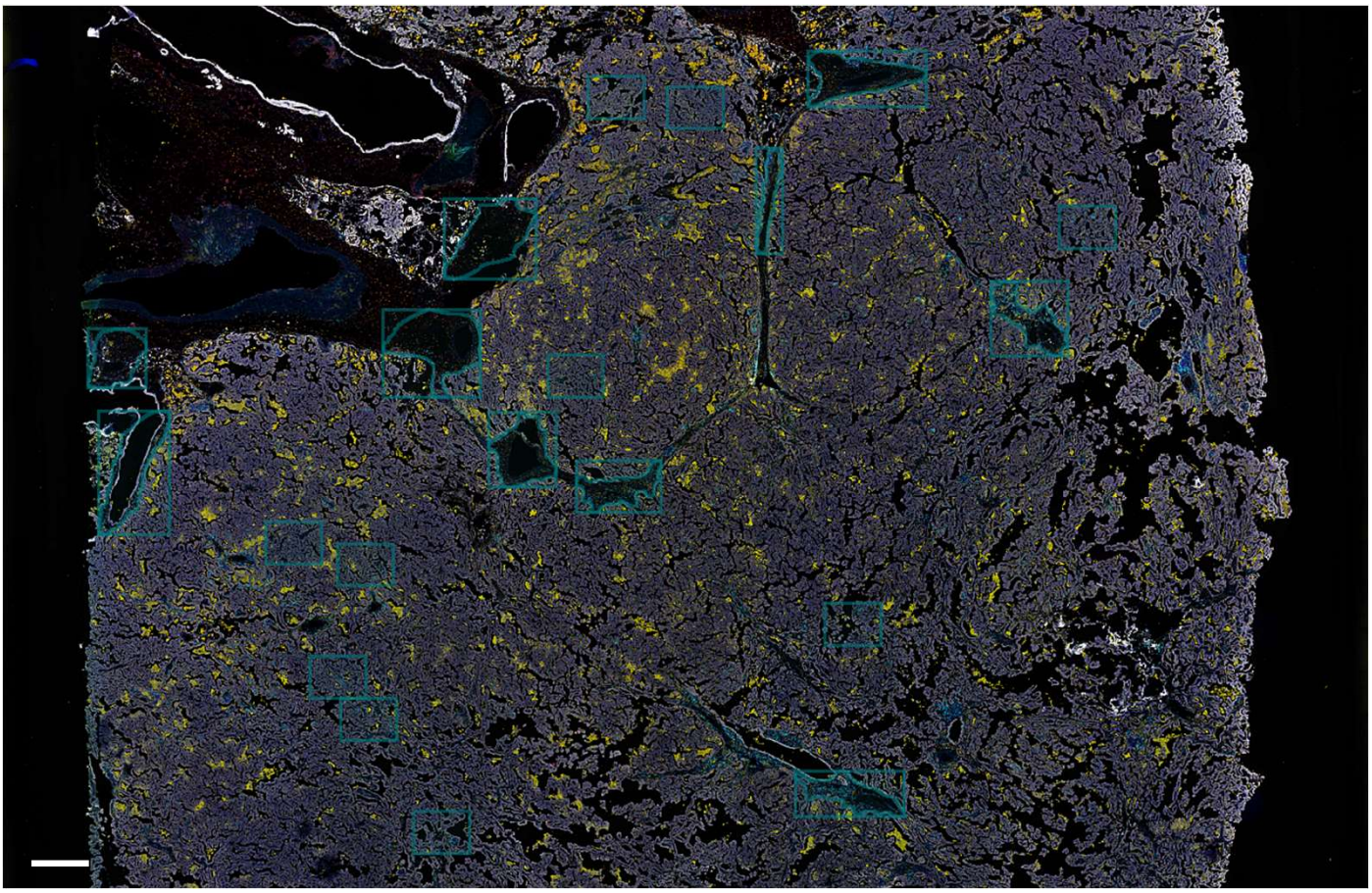

Fig. S6 (Cont'd)

Fig. S6 Tissue slide images of the representative cases (KNUCH03, Solid group; KNUCH22, A/P group).

A Whole-slide H&E image of KNUCH03. The tumor area confirmed by pathologists is outlined in red. **B,C** Multiplex IHC images of KNUCH03. In **B**, the orange box indicates the area shown in **C**. In **C**, the yellow and green boxes correspond to the regions shown in Fig. 4A and C, respectively. **D** Whole-slide H&E image of KNUCH22. The tumor area confirmed by pathologists is outlined in red. **E,F** Multiplex IHC images of KNUCH22. In **E**, the orange box indicates the area shown in **F**. In **F**, the yellow box corresponds to the region shown in Fig. 4B. **G,H** ROIs in the multiplex IHC images of KNUCH03 and KNUCH22, respectively. A total of 20 ROIs (10 within the tumor nest and 10 within the peritumoral stroma) were selected per sample using Phenochart software. Scale bars: 4mm (**A,B,D,** and **E**); 1mm (**C,F,G,** and **H**).

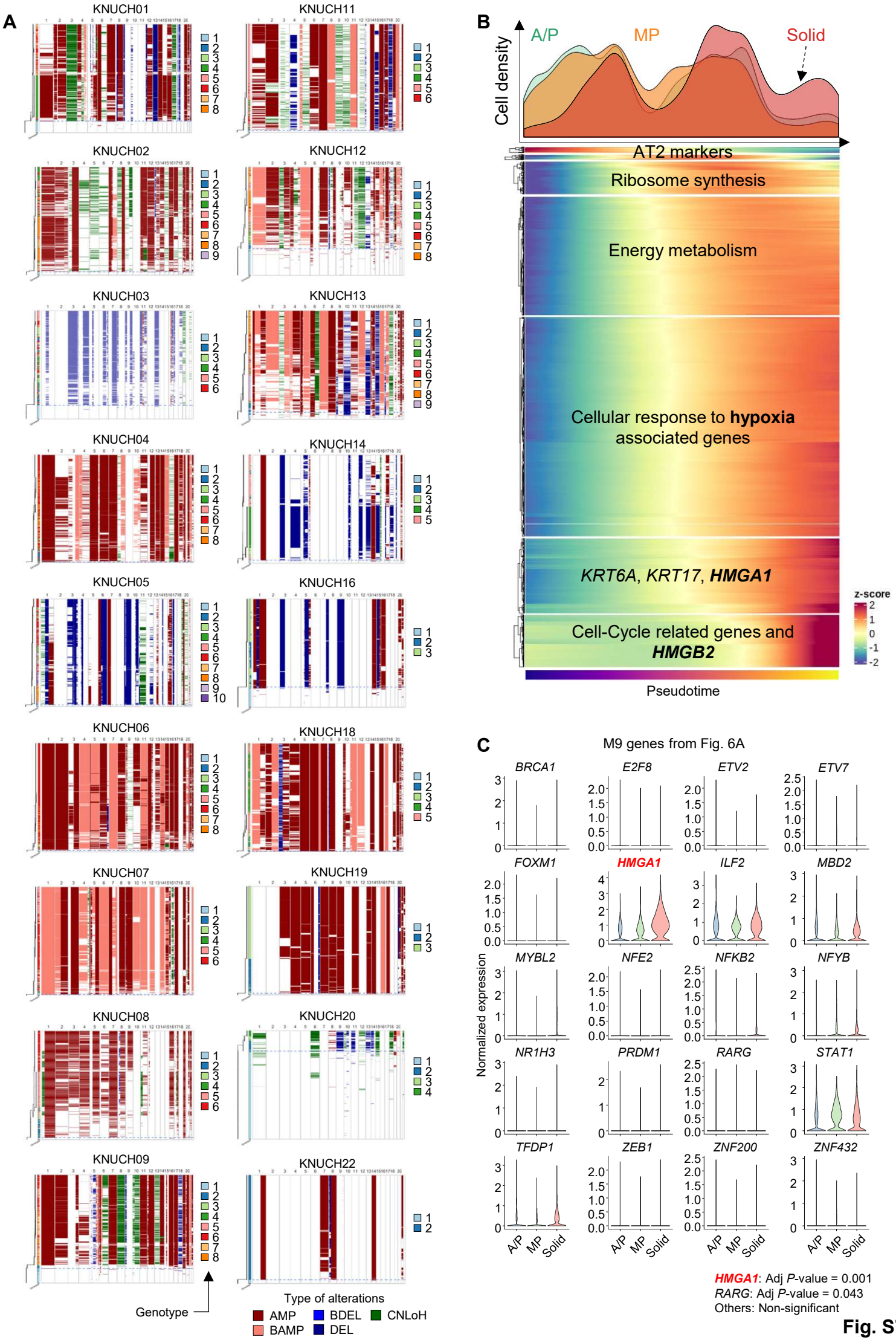
A
KNUCH01
KNUCH11
KNUCH02
KNUCH12
KNUCH03
KNUCH13
KNUCH04
KNUCH14
KNUCH05
KNUCH16
KNUCH06
KNUCH18
KNUCH07
KNUCH19
KNUCH08
KNUCH20
KNUCH09
KNUCH22
Genotype
Type of alterations
AMP
BAMP
BDEL
DEL
CNLoH
B
Cell density
A/P
MP
Solid
AT2 markers
Ribosome synthesis
Energy metabolism
Cellular response to hypoxia associated genes
KRT6A, KRT17, HMGA1
Cell-Cycle related genes and HMGB2
Pseudotime
z-score
C
M9 genes from Fig. 6A
BRCA1
E2F8
ETV2
ETV7
FOXM1
HMGA1
ILF2
MBD2
MYBL2
NFE2
NFKB2
NFYB
NR1H3
PRDM1
RARG
STAT1
TFDP1
ZEB1
ZNF200
ZNF432
Normalized expression
A/P
MP
Solid
HMGA1: Adj P-value = 0.001
RARG: Adj P-value = 0.043
Others: Non-significant

Fig. S7

Fig. S7 Cancer cell identification and transcriptomic dynamics across histologic subtype groups.

A Heatmaps displaying patient-specific copy number variation (CNV) patterns inferred by Numbat for cancer cell identification. **B** Heatmap showing dynamically expressed genes across pseudotime estimated by Monocle3. The top panel shows the density of cancer cells in each histologic subtype group across pseudotime. **C** Violin plots showing expression of transcription factors associated with the Solid group regulon module (M9) as shown in Fig. 6A.

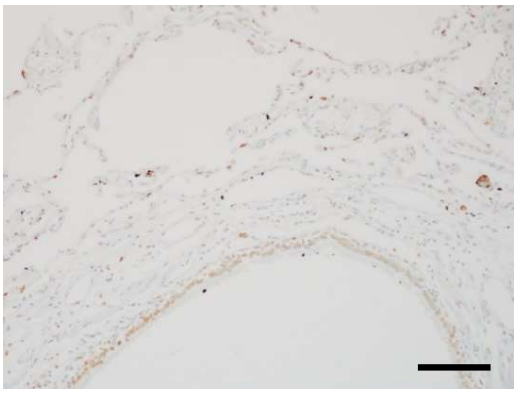
A
Normal bronchiolar epithelium

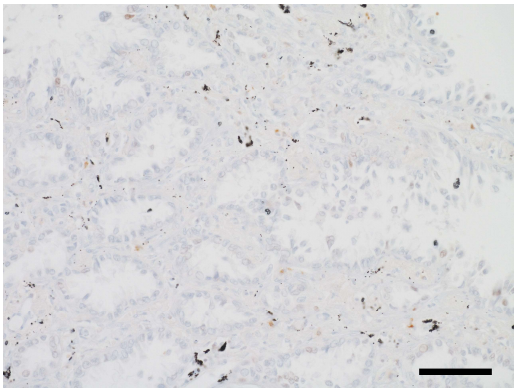
B

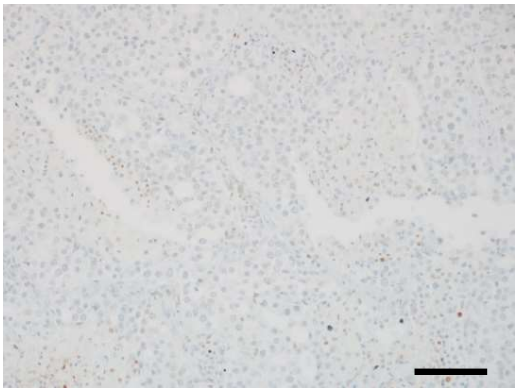
F
0

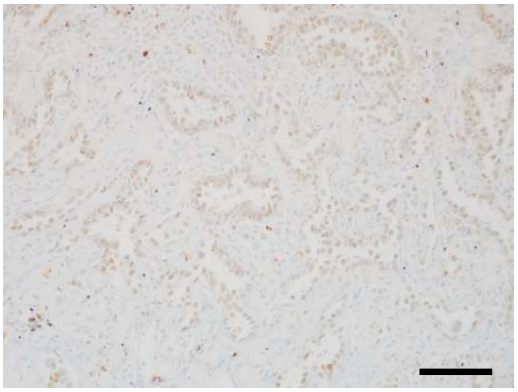
C

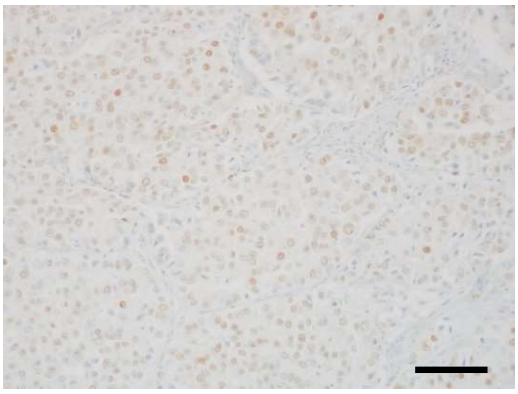
G
1+

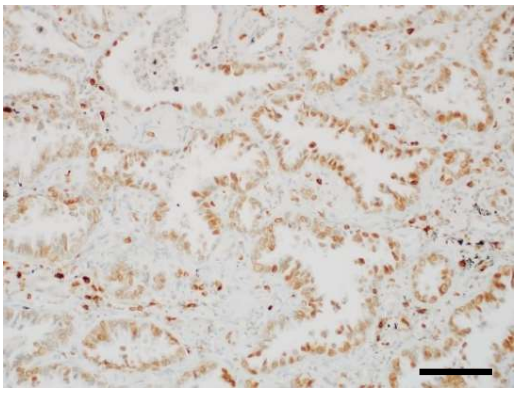
D

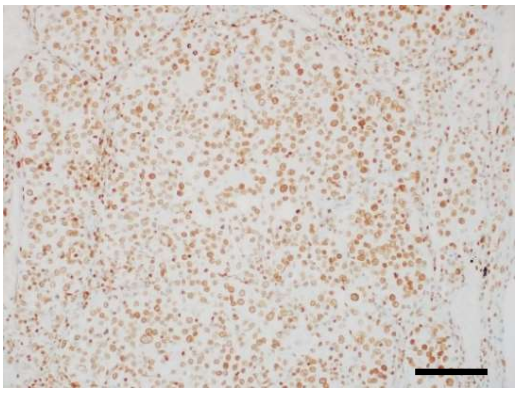
H
2+

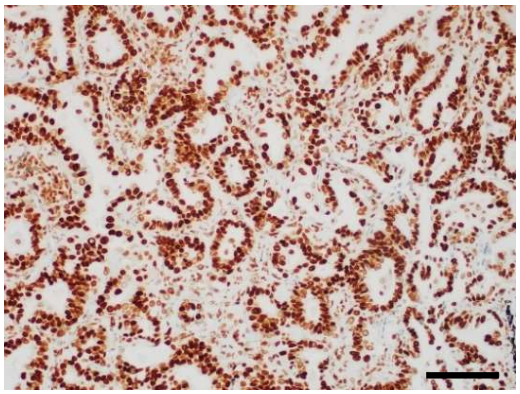
E
Acinar pattern

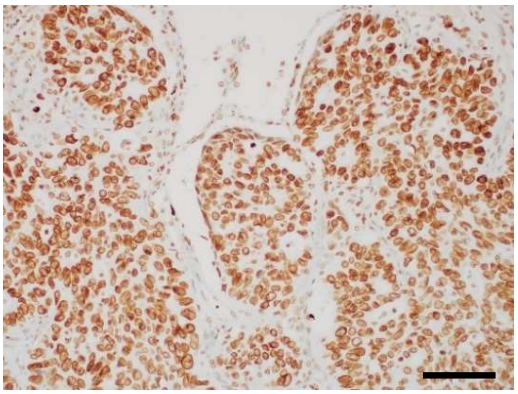
I
3+
Solid pattern

Fig S8

Fig. S8 HMGA1 immunohistochemistry showing variable levels of HMGA1 nuclear positivity (magnification, ×200).

HMGA1 protein expression was highly heterogeneous within individual tumors. Both solid-dominant and non-solid areas on the same slide frequently showed variable HMGA1 nuclear positivity; in some cases, certain acinar-pattern regions exhibited higher expression than adjacent solid-pattern regions within the same tumor. Despite such intratumoral heterogeneity, HMGA1 expression, quantified as the percentage of tumor cells showing nuclear staining on each whole slide, was significantly higher in Solid group tumors than in A/P group tumors. These findings indicate that upregulation of HMGA1 is a characteristic feature of tumors belonging to the Solid group. **A** Normal bronchiolar epithelium. **B–E** Lung adenocarcinoma with an acinar pattern. **F–I** Lung adenocarcinoma with a solid pattern. Scale bar, 50μm.

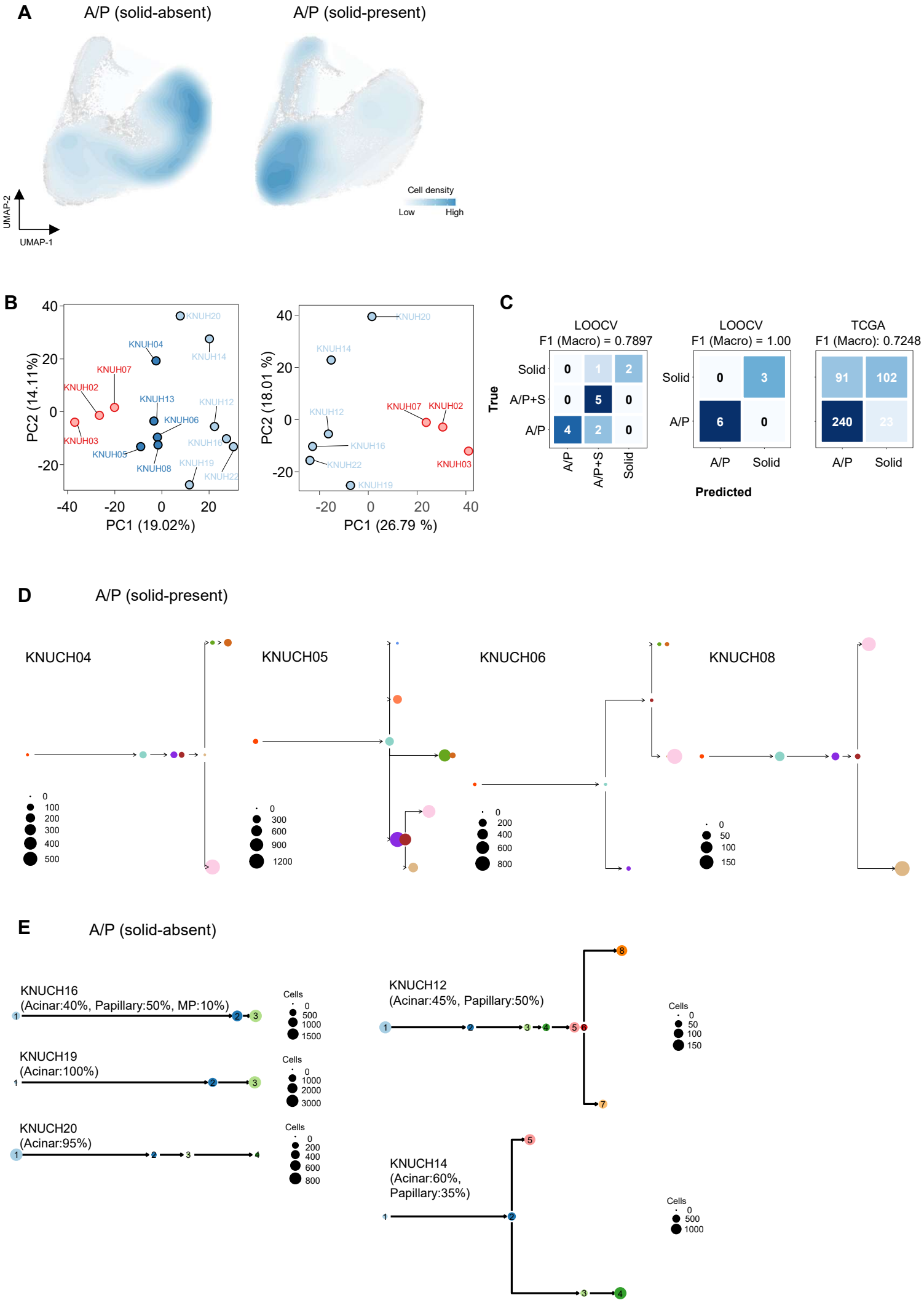
A
A/P (solid-absent)
A/P (solid-present)
UMAP-2
UMAP-1
Cell density
Low
High
B
PC2 (14.11%)
PC1 (19.02%)
PC2 (18.01 %)
PC1 (26.79 %)
KNUH20
KNUH04
KNUH14
KNUH07
KNUH02
KNUH13
KNUH12
KNUH06
KNUH03
KNUH16
KNUH05
KNUH08
KNUH19
KNUH22
C
LOOCV
F1 (Macro) = 0.7897
LOOCV
F1 (Macro) = 1.00
TCGA
F1 (Macro): 0.7248
True
Solid
A/P+S
A/P
Predicted
D
A/P (solid-present)
KNUCH04
KNUCH05
KNUCH06
KNUCH08
E
A/P (solid-absent)
KNUCH16
(Acinar:40%, Papillary:50%, MP:10%)
KNUCH19
(Acinar:100%)
KNUCH20
(Acinar:95%)
KNUCH12
(Acinar:45%, Papillary:50%)
KNUCH14
(Acinar:60%,
Papillary:35%)
Cells

Fig. S9

Fig. S9 Presence of solid component influences intratumor heterogeneity in A/P group LUAD.

A UMAP plots showing cancer cell density in solid-absent A/P (left) and solid-present A/P (right) tumors. **B** PCA of pseudobulk scRNA-seq expression profiles of cancer cells. Left: three-class classifier samples (A/P [solid-absent A/P], A/P+S [solid-present A/P] and Solid; n = 14). Right: binary classifier samples (A/P vs. Solid; n = 9). The proportion of variance explained is indicated on each axis. **C** Confusion matrices summarizing classifier performance. Left: LOOCV of the three-class multinomial logistic regression classifier (F1 = 0.79). Middle: LOOCV of the binary logistic regression classifier showing complete separation of A/P and solid tumors (F1 = 1.00). Right: external validation on TCGA-LUAD bulk RNA-seq data (n = 456; 263 A/P, 193 Solid; F1 = 0.72). **D,E** Phylogenetic trees of cancer cells from solid-present (**D**) and solid-absent (**E**) A/P tumors.

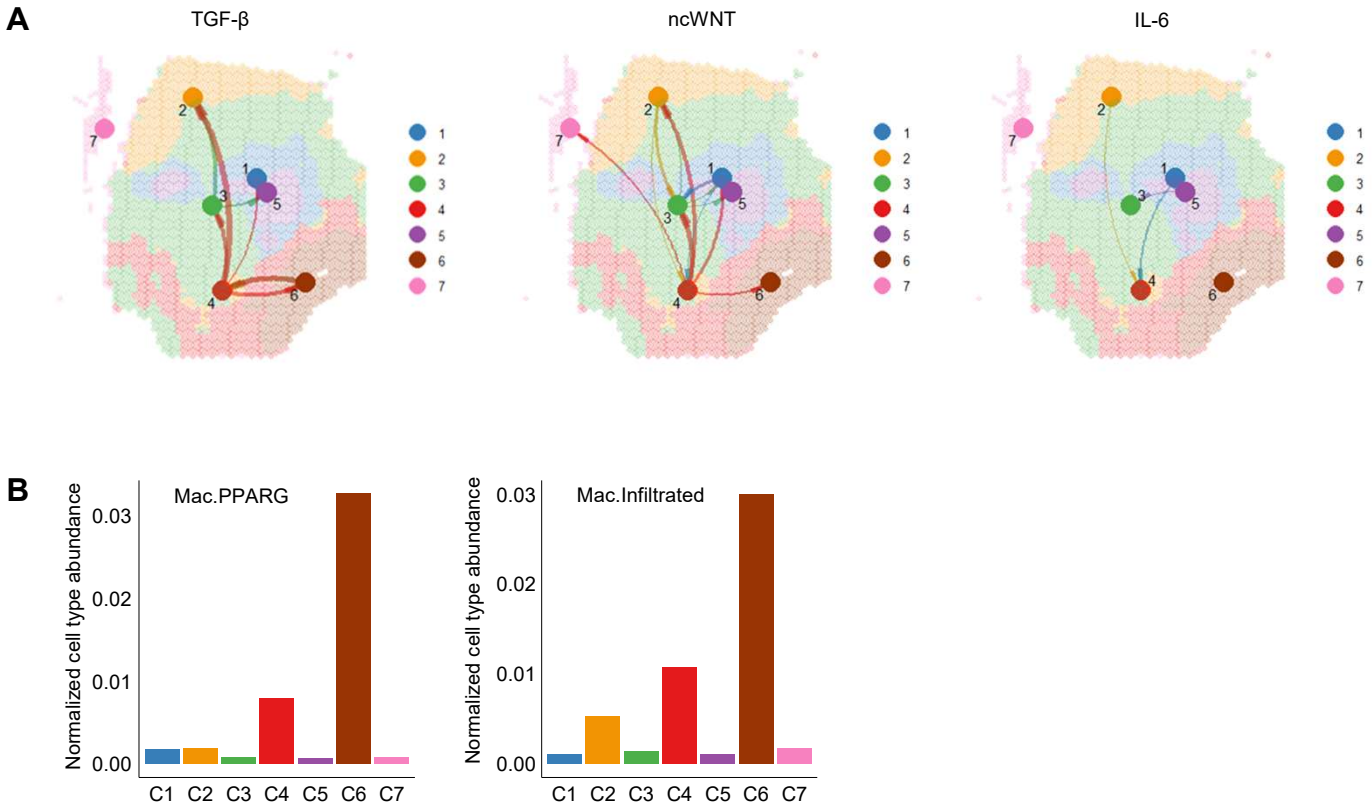

Fig. S10 Spatial ligand–receptor interaction analysis using CellChat in Solid group LUAD.

A Ligand–receptor interaction signaling enriched in solid group tumor (KNUCH23) inferred by CellChat. **B** Normalized relative abundance of macrophage subtypes across spatial clusters.

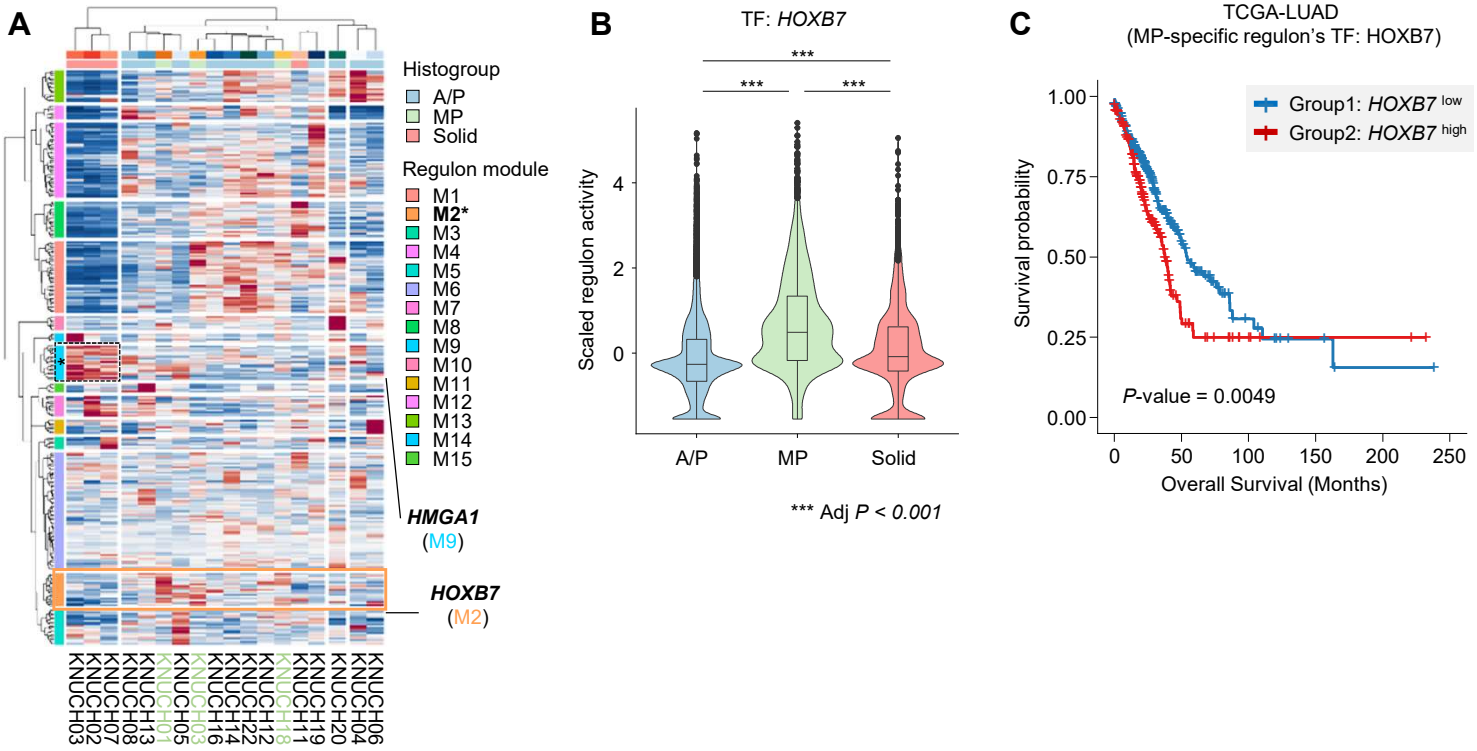

Fig. S11: MP-specific regulon module and *HOXB7* prognostic significance in LUAD.

A Heatmap showing regulon activities predicted by SCENIC in cancer cells, averaged per patient, highlighting the MP-specific regulon module (M2). **B** Violin plot showing *HOXB7* regulon activity in cancer cells across histologic subtype groups. **C** Kaplan–Meier survival curves showing prognostic significance of *HOXB7* expression in the TCGA-LUAD cohort.